Magnetized plasma flows and magnetoplasmadynamic thrusters

Cite as: Phys. Plasmas **17**, 063507 (2010); https://doi.org/10.1063/1.3447876
Submitted: 04 February 2010 . Accepted: 14 May 2010 . Published Online: 25 June 2010

T. Andreussi, and F. Pegoraro

Magnetized plasma flows and magnetoplasmadynamic thrusters

T. Andreussi[1,a)] and F. Pegoraro[2,b)]
[1]*Department of Aerospace Engineering, Pisa University, 56122 Pisa, Italy*
[2]*Department of Physics, Pisa University and CNISM, 56127 Pisa, Italy*

(Received 4 February 2010; accepted 14 May 2010; published online 25 June 2010)

An axisymmetric magnetohydrodynamics (MHD) model of the acceleration channel of an applied-field magnetoplasmadynamic thruster is presented. A set of general relationships between the flow features and the thruster performance is obtained. The boundary conditions and the flow regime, which depends on the Alfvén Mach number, are shown to provide the ideal limits of steady state thruster operation. In the present analysis, a Hamiltonian formulation of the MHD plasma flow model is adopted. This formulation makes it possible to cast the model equations in a variational form, which is then solved by using a finite element numerical algorithm. © *2010 American Institute of Physics*. [doi:10.1063/1.3447876]

I. INTRODUCTION

The study of the flow of a conductive fluid or of a plasma is fundamental for a broad class of physical and technological problems. In magnetic confinement fusion experiments, significant modifications of the plasma equilibrium configuration and stability are known to be caused by plasma flows. Astrophysical phenomena, such as stellar winds and accretion disks, represent a research area where the properties of plasma flows play a basic role. In addition, the properties of plasma flows are of basic importance for those technologies, such as electric propulsion and plasma generators that specifically aim at converting electromagnetic energy into kinetic energy or vice versa. Research on electric propulsion started at the beginning of the past century (see Ref. 1) and now electric thrusters represent an advanced technology solution for space maneuvering.

The behavior of a plasma flow depends on the interaction between the electromagnetic fields and the conducting medium. This interaction, which in most cases involves nonstationary fields and dissipation through viscous and resistive effects, leads to a highly complex model. By neglecting dissipative effects and assuming plasma quasineutrality, a general, although simplified, description of the main acceleration processes is possible within the framework of the ideal magnetohydrodynamics (MHD) model. If in addition the flow configuration is assumed to be time independent and axisymmetric, the MHD equations reduce to a generalized form of the Grad–Shafranov[2–4] equation, which is used to describe static plasma equilibria in magnetic confinement experiments, and of the Bragg–Hawthorne[5–9] equation for a hydrodynamic flow with swirl.

The equations that describe these generalized axisymmetric MHD plasma equilibria with flows[10] (in the following called generalized equilibria for short) can be expressed either in terms of a magnetic flux function or of a mass flux function. The structure of the plasma configuration is found to depend on five flux functions and can be obtained by solving, with the appropriate boundary conditions, a second order nonlinear partial differential equation (PDE). As shown in Refs. 10 and 11 this equation can present three points of transition, each with a corresponding class of shock discontinuities,[12] which depend on the Alfvén Mach number. The nonlinear dependence of the coefficients of this PDE on the flux functions and the change in its differential nature at the transition points complicates its explicit solution.

Due to the nondissipative nature of this model, a noncanonical Hamiltonian formulation[13–17] can be adopted as it allows us to overcome some of the difficulties inherent in the differential formulation by using the Hamiltonian as a variational functional constrained by four "flow invariants" (called Casimirs, see below). In fact, a variational principle associated with generalized equilibria was reported in Heinemann and Olbert[18] and developed by Hameiri[19] and Goedbloed.[11] In Ref. 20 the general set of Casimir invariants was derived and in Ref. 21 the Casimirs and the Hamiltonian dynamics of axisymmetric plasma flows are presented in terms of noncanonical Poisson bracket. In Ref. 21 the equations describing generalized equilibria are presented in both MHD and hydrodynamic forms and the corresponding variational principles are explicitly deduced. As shown by the authors,[22] this variational approach can be extended so as to include open-boundary conditions and discontinuous solutions.

As pointed out above, plasma flows are a fundamental feature for different configurations in plasma and space physics research and applications. As long as the axisymmetry and stationarity conditions hold, MHD problems (such as the structure of astrophysical jets[9,23–26] or the description of toroidal equilibria of magnetized plasmas with flows[27] of interest for thermonuclear fusion experiments) can be treated within the approach discussed in the present paper. In the following, we will focus our attention on electric thruster technology. This technology offers a suitable ground for studying plasma acceleration and represents the main aim of an internationally widespread research program and experimental campaign. More specifically, in the present paper we will examine the acceleration processes of a simple thruster

a)Electronic mail: t.andreussi@alta-space.com.
b)Electronic mail: pegoraro@df.unipi.it.

configuration, a magnetoplasmadynamic (MPD) thruster with an applied magnetic field by using a stationary axisymmetric ideal MHD mode (a description of this thruster configuration can be found in Refs. 28 and 29).

An introduction to the model adopted and to its variational formulation is presented in Sec. II. In Sec. III an open boundary plasma acceleration channel is described and some general properties of the thruster performance are deduced. From the study of these generalized equilibria, we obtain the ideal limits of the steady state thruster operation regime, which provide fundamental information for thruster design. A numerical procedure based on the variational approach is presented in Sec. IV, where the Ritz method described and validated in Ref. 22 is extended via a finite elements formulation in order to treat complex configurations. In the same section the numerical results obtained for thruster configurations are presented. Finally, in Sec. V we discuss the main results of the present investigation and possible developments of the numerical analysis.

II. MAGNETIZED PLASMA FLOWS

A. Generalized equilibria

The MHD stationary plasma flows are described by the equations

$$\nabla \cdot (\rho \mathbf{v}) = 0, \tag{1}$$

$$\rho(\mathbf{v} \cdot \nabla)\mathbf{v} = -\nabla p + \frac{1}{c}\mathbf{j} \times \mathbf{B}, \tag{2}$$

$$\mathbf{v} \cdot \nabla S = 0, \tag{3}$$

where ρ and S are the plasma density and entropy, $\mathbf{v}$ represents the flow velocity, and c is the speed of light. The pressure p can be expressed in terms of the plasma internal energy per unit mass $U=U(\rho,S)$ as $p=\rho^2(\partial U/\partial\rho)$ and, from the entropy equation, we can deduce

$$\rho^{-1}\nabla p = \nabla I - \Theta \nabla S, \tag{4}$$

where $I(p,S)=U+p/\rho$ is the plasma enthalpy per unit mass and $\Theta=\partial U/\partial S$ is the plasma temperature. In addition, the current density $\mathbf{j}$ and the magnetic field $\mathbf{B}$ that define the Lorentz force in the momentum equation (2) satisfy Ampére's law, Faraday's law, and the perfect conductivity equation

$$\nabla \times \mathbf{B} = \frac{4\pi}{c}\mathbf{j}, \quad \nabla \times \mathbf{E} = 0, \tag{5}$$

$$\mathbf{E} + \frac{1}{c}\mathbf{v} \times \mathbf{B} = 0, \tag{6}$$

where $\mathbf{E}$ is the electric field.

In order to treat axisymmetric equilibria, we introduce a cylindrical coordinate system (r,ϕ,z), where the azimuthal angle ϕ is the ignorable coordinate and ϕ=const defines a poloidal plane. Moreover, in the following, $\hat{\phi}$ represents the unit vector in the azimuthal direction and the subscript ϕ indicates the azimuthal component of the magnetic field B_ϕ and of the plasma velocity v_ϕ. Being divergence-free, the poloidal component of the magnetic field can be expressed as

$$\mathbf{B}_p = \nabla\psi \times \nabla\phi, \tag{7}$$

where the scalar function ψ, which labels magnetic flux surfaces, is called the magnetic flux function. The mass conservation equation [Eq. (1)] implies a similar representation for the poloidal mass flow

$$\rho\mathbf{v}_p = \nabla\chi \times \nabla\phi, \tag{8}$$

where χ is the flux function of the mass flow. From the azimuthal component of Eq. (6), it follows that

$$\nabla\psi \times \nabla\chi = 0 \tag{9}$$

so the two flux functions, ψ and χ, are functionally dependent.

In a purely hydrodynamic problem, the magnetic flux function is constant and the problem is expressed in terms of χ. The momentum equation in the direction of $\nabla\chi$ can be written as

$$\nabla \cdot \left(\frac{1}{\rho}\frac{\nabla\chi}{r^2}\right) = \rho\frac{dB}{d\chi} - \rho\frac{C}{r^2}\frac{dC}{d\chi} - \rho\Theta\frac{dS}{d\chi}, \tag{10}$$

where B represents the *Bernoulli function* $B=(1/2)v^2+I$ and $C=rv_\phi$ is the angular momentum per unit mass about the symmetry axis. Both these functions and the fluid entropy are constants on each streamline and thus, in stationary conditions, can be expressed as functions of χ. In general, the fluid density that appears in Eq. (10) is a nontrivial function of χ and its derivatives. This functional dependence can be deduced from the Bernoulli function

$$B(\chi) = \frac{1}{2}\left(\frac{\nabla\chi}{\rho r}\right)^2 + \frac{1}{2}\left[\frac{C(\chi)}{r}\right]^2 + I[\rho,S(\chi)] \tag{11}$$

but, in general, it is not possible to determine an explicit relationship $\rho=\rho(\mathbf{x},\chi,\nabla\chi)$. However, for incompressible flows Eq. (10), known as the Bragg–Hawthorne equation, is formally identical to the Grad–Shafranov equation, which has been widely investigated in order to obtain static plasma equilibria.

Since the generalized equilibria model follows from the studies on the Grad–Shafranov equation, the function ψ is often preferred and Eq. (9) is rewritten as

$$\chi = \chi(\psi). \tag{12}$$

In fact, this implies a monotonicity constraint on ψ and thus restricts the possible solutions. However, from the point of view of the plasma dynamics, the choice between the two flux functions, ψ and χ, is not equivalent because Eq. (8) is no longer valid if $\partial\rho/\partial t \neq 0$ and the dynamic invariants cannot be expressed as functions of χ (see Ref. 21).

From the equations of the model, a set of five flux functions follows that represent quantities conserved along streamlines

$$F(\psi) = 4\pi\chi', \tag{13}$$

$$G(\psi) = (v_\phi - v_p B_\phi/B_p)/r, \tag{14}$$

$$H(\psi) = rB_\phi - rFv_\phi, \tag{15}$$

$$J(\psi) = v^2/2 + I - rv_\phi G, \tag{16}$$

$$S(\psi) = S, \tag{17}$$

where J is a generalization of the Bernoulli function and a prime indicates derivation with respect to ψ. Thus, the equation for the generalized equilibria reads as

$$\nabla \cdot \left[\left(\frac{F^2}{4\pi\rho} - 1 \right) \frac{\nabla\psi}{r^2} \right] - \frac{FF'}{4\pi\rho} \left(\frac{|\nabla\psi|}{r} \right)^2 = 4\pi\rho(J' + rv_\phi G' - \Theta S') + \frac{B_\phi}{r}(H' + rv_\phi F'), \tag{18}$$

where the plasma density is related to ψ and its derivatives through the implicit Bernoulli equation.

The dimensionless parameter $M^2 = F^2/4\pi\rho$ is the square of the Alfvén Mach number, which characterizes the second order PDE (18). As discussed in Refs. 10 and 11, the equation for the generalized equilibria is hyperbolic for $M_c^2 \le M^2 \le M_s^2$ and for $M^2 \ge M_f^2$, where $M_c^2 \equiv \gamma p/(\gamma p + B^2/4\pi)$ is the square Alfvén Mach number corresponding to the "cusp velocity"[30] and

$$M_{f,s}^2 \equiv \frac{4\pi\gamma p + B^2}{2B_p^2} \left\{ 1 \pm \left[1 - \frac{16\pi\gamma p B_p^2}{(4\pi\gamma p + B^2)^2} \right]^{1/2} \right\} \tag{19}$$

are the square Alfvén Mach numbers relative to the slow and fast magnetosonic velocities, respectively, M_s^2 and M_f^2.

B. Variational formulation

As described in Refs. 13–17 and 21, a Hamiltonian formulation of the hydrodynamic and MHD equations is possible in terms of a noncanonical Poisson bracket

$$\{\mathcal{F}, \mathcal{G}\} = \int_V \left(\frac{\delta\mathcal{F}}{\delta\eta_i} \Im_{ij} \frac{\delta\mathcal{G}}{\delta\eta_j} \right) d^3r, \tag{20}$$

where $\mathcal{F}$ and $\mathcal{G}$ are two functionals and $\delta\mathcal{F}/\delta\eta_i$ represents a functional derivative. The noncanonical Poisson bracket $\{\cdot,\cdot\}$ satisfies the antisymmetry condition and the Jacobi identity and $\Im$ is a bilinear skew-symmetric operator, which is called the *cosymplectic operator* (the complete expression of $\Im$ for the axisymmetric MHD case can be found in Ref. 21). The dynamics of the Eulerian variables $\eta = \{\rho, \mathbf{v}_p, v_\phi, \psi, B_\phi, S\}$ can be written as

$$\frac{\partial\eta}{\partial t} = \{\eta, \mathcal{H}\}, \tag{21}$$

where the Hamiltonian

$$\mathcal{H} = \frac{1}{2} \int_V \left(\rho v^2 + \frac{B^2}{4\pi} + 2\rho U \right) d^3r \tag{22}$$

is the total energy of the system. Since the Eulerian representation is noncanonical, it is possible to find a set of dynamic invariants, which are called Casimir invariants that satisfy

$$\{\mathcal{C}, \mathcal{F}\} = 0 \tag{23}$$

for all functionals $\mathcal{F}$. The functionals $\mathcal{C}$ are determined by the noncanonical Poisson bracket alone and if we assume the entropy equation $S = S(\psi)$, for the axisymmetric MHD, we obtain

$$\mathcal{C}_1 = \int_V \rho J(\psi) d^3r, \tag{24}$$

$$\mathcal{C}_2 = \int_V \frac{B_\phi}{r} H(\psi) d^3r, \tag{25}$$

$$\mathcal{C}_3 = \int_V r\rho v_\phi G(\psi) d^3r, \tag{26}$$

$$\mathcal{C}_4 = \int_V \mathbf{v} \cdot \mathbf{B} F(\psi) d^3r, \tag{27}$$

where F, G, H, and J are generic functions of ψ. From the condition (23), it follows that the constrained Hamiltonian

$$\mathcal{E} = \mathcal{H} - \int \rho J(\psi) - \int \frac{1}{4\pi r} B_\phi H(\psi) - \int r\rho v_\phi G(\psi) - \int (\mathbf{v} \cdot \mathbf{B}) F(\psi) \tag{28}$$

generates the same dynamics as Eq. (21), and thus equilibria are obtained for

$$\frac{\delta\mathcal{E}}{\delta\eta_j} = 0. \tag{29}$$

In fact, by taking the variations of $\mathcal{E}$ with respect to the variables η_j we see that the generalized equilibria equations correspond to the extrema of the constrained Hamiltonian and that the dynamic invariants generate the set of flux functions (13)–(16) of the generalized equilibria model (except for the entropy equation, which is an assumption of the Hamiltonian formulation).

The variational principle (28) depends on the whole set of variables $\eta = \{\rho, \mathbf{v}_p, v_\phi, \psi, B_\phi\}$ but can be simplified by substituting a variable with the expression obtained from the corresponding variation. For example, the variation of $\mathcal{E}$ with respect to $\mathbf{v}_p$ gives

$$\frac{\delta\mathcal{E}}{\delta\mathbf{v}_p} = \mathbf{v}_p - F\mathbf{B}_p \rightarrow \mathbf{v}_p = F\nabla\psi \times \nabla\phi. \tag{30}$$

This equation can be substituted into Eq. (28) in order to reduce the number of variables. However, since the Bernoulli equation is an implicit equation for ρ, the plasma density needs to be treated as an independent variable. Furthermore, although the azimuthal velocity can be written in the explicit form

$$rv_\phi = \left(r^2 G + \frac{FH}{4\pi\rho} \right) \left(1 - \frac{F^2}{4\pi\rho} \right)^{-1}, \tag{31}$$

this expression presents a possible singularity for $M = 1$ and its substitution complicates the solution procedure. Thus, we

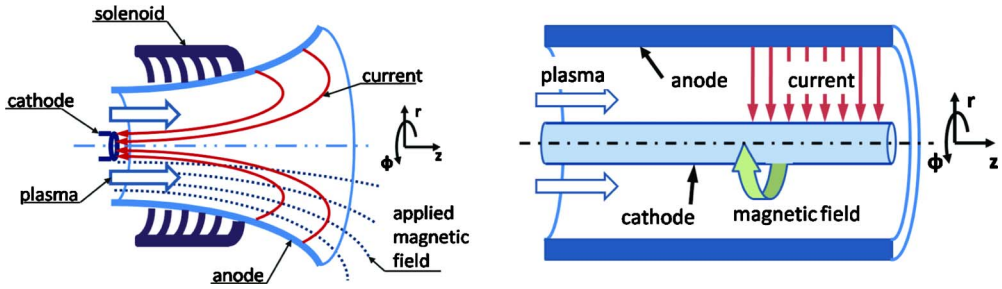

FIG. 1. (Color online) Applied-field MPD thruster configuration (left frame) and self-field MPD thruster configuration (right frame).

maintain the dependence on the azimuthal velocity and write the variational principle as a functional of three independent variables in the form

$$\mathcal{L}(v_\phi,\rho,\psi) = -\int_V \left[\left(\frac{F^2}{4\pi\rho}-1\right)\frac{1}{8\pi}\left(\frac{\nabla\psi}{r}\right)^2 + \frac{1}{8\pi}\left(\frac{H+4\pi r v_\phi F}{r}\right)^2 - \frac{1}{2}\rho v_\phi^2 + \rho(J+rv_\phi G) - \rho U\right] d^3r. \tag{32}$$

In the foregoing treatment of both the variational and the differential formulations of the problem, boundary conditions were not specified. For closed geometries, which are typical of magnetic confinement configurations, the boundary is defined by a magnetic flux surface and the corresponding condition is ψ=const on the boundary. However, in order to study the acceleration processes in a plasma thruster, which is a open-boundary problem, we need a description of the thruster configuration that includes the inlet and the outlet regions. This description and the consequent discussion on the boundary conditions are subjects of Sec. III.

III. MPD THRUSTERS

The mathematical approach developed in the previous sections can be used in order to construct explicit solutions of the MHD equations that describe the acceleration channel of an applied-field MPD thruster, see description below, and to formulate the appropriate boundary conditions at the exit of the acceleration channel. In addition, the formulation of the governing equations in terms of flux functions allows us to obtain general relationships between the features of the plasma flow and the thruster performance.

A. Thruster description and steady state regime

Figure 1 shows the typical geometry of an applied-field MPD thruster.[28,29] This thruster configuration consists of an injection region with a central electrode (cathode) and a divergent conductive wall that constitutes the second electrode (anode). A solenoid generates a poloidal magnetic field that is shaped by the conductive nozzle. A neutral gas (the most common gases used as propellants for this kind of plasma thrusters are argon, xenon, or lithium) is ionized by a strong electric field and by electrons emitted through the cathode. The plasma enters the acceleration channel and the current flows from the wall trough the plasma and up to the injection region and the cathode. The poloidal current generates an azimuthal magnetic field, which accelerates the plasma through the Lorentz force term in the plasma momentum equation.

For the special case of a coaxial self-field plasma accelerator, with no applied poloidal magnetic field, a simplified quasi-one-dimensional analysis of the mass and of the momentum conservation equations is possible. In this case the magnetic field is in the azimuthal direction only and is generated by the current that flows through the central cathode. Hence, at the inlet (indicated by the subscript i) the magnetic field is given by

$$B_{\phi i} = 2I_{\mathrm{tot}}/(cr),$$

where I_{tot} is the total current that flows through the electrodes. Assuming that the axial plasma velocity v_z is uniform over each channel section orthogonal to the symmetry axis, the momentum equation yields the Maecker formula[31,32] for the thrust T,

$$T = \dot{m}[\![v_z]\!] = \left(\frac{I_{\mathrm{tot}}}{c}\right)^2\left(\ln\frac{r_a}{r_c}+A\right), \tag{33}$$

where $\dot{m}$ is the assigned propellant mass flow rate, $[\![v_z]\!]=(v_{zo}-v_{zi})$ indicates the difference between the outlet and the inlet mean axial velocity, r_a and r_c represent the effective radii of the anode and the cathode, and A is a parameter that depends on the current pattern, on the pressure distribution, and on the electrode geometry (an accurate analysis of these dependencies for real thruster configurations can be found in Ref. 32). Neglecting the pressure term in the momentum equation in comparison with the electromagnetic term, for cylindrical electrodes (sketched in Fig. 1), the parameter A in Eq. (33) vanishes. In this latter case, from the energy balance, it follows that

$$\tfrac{1}{2}\dot{m}[\![v_z^2]\!] = I_{\mathrm{tot}}\Delta V, \tag{34}$$

where ΔV is the overall potential difference between the two electrodes and $[\![v_z^2]\!]$ represents the difference of the square velocity which can be rewritten in the form

$$[\![v_z^2]\!] = [\![v_z]\!](2v_{zi}+[\![v_z]\!]). \tag{35}$$

The inlet velocity can either be taken to be negligible with respect to the velocity increment or can be considered to be of the same order. In both cases by combining Eqs. (33) and (34) we obtain a cubic relationship between the current I_{tot}

and the potential difference ΔV. Equations (33) and (34) were obtained, assuming that the propellant is completely ionized at the inlet of the acceleration channel, thus neglecting the energy losses due to the ionization of the gas and the acceleration processes in the ionization region. In fact, it is known that in the low current regimes the ionization process limits the effective thrust. Moreover, until complete ionization of the propellant is reached, the plasma velocity is limited by the presence of a neutral flow at the critical ionization velocity

$$v_{\rm crit} = \sqrt{2E_{\rm ion}/\mathsf{M}}, \tag{36}$$

where $E_{\rm ion}$ is the ionization energy of the propellent and M represents its atomic mass.

In the derivation of Eq. (34) no equation for the plasma conductivity need be considered. If a perfect plasma conductivity [see Eq. (6)] is a reasonable assumption in the region where the propellant is completely ionized (i.e., at the inlet of the acceleration channel), Eq. (6) gives

$$\left.\frac{\partial V}{\partial r}\right|_i = -\frac{1}{c} v_{zi} B_{\phi i} = v_{zi} \frac{2I_{\rm tot}}{c^2 r}. \tag{37}$$

Integrating Eq. (37) from the cathode to the anode radius and substituting the potential difference into Eq. (34), we obtain

$$\frac{1}{2}\dot{m}[\![v_z^2]\!] = 2v_{zi}\left(\frac{I_{\rm tot}}{c}\right)^2 \ln\frac{r_a}{r_c} \tag{38}$$

and the comparison with the Maecker formula yields

$$2v_{zi} = [\![v_z]\!]. \tag{39}$$

Since the inlet velocity v_{zi} is limited by the critical ionization velocity, the obtainable thrust is limited by

$$T \le 2\dot{m} v_{\rm crit}. \tag{40}$$

Hence, an important thruster operation parameter is defined by the ratio

$$\xi = \frac{[\![v_z]\!]}{v_{\rm crit}} = \left(\frac{I_{\rm tot}}{c}\right)^2 \frac{\ln(r_a/r_c) + A}{\dot{m}\sqrt{2E_{\rm ion}/\mathsf{M}}} \tag{41}$$

and the normal operation regimes are in the interval

$$0 \le \xi \le 2, \tag{42}$$

which represents the ideal limits of *steady state* thruster operation. We note that although the above analysis is based on self-field plasma accelerators, similar considerations can be used to treat the case of the applied-field MPD thruster.

B. Boundary conditions

The conductive wall and the axis of the (axisymmetric stationary) thruster are two flux surfaces. In order to simplify the following analysis, we consider a conic nozzle (Fig. 2) and we introduce a set of spherical coordinates (σ, θ, ϕ), where ϕ is the ignorable coordinate.

The boundary conditions on the axis and on the wall can thus be expressed as

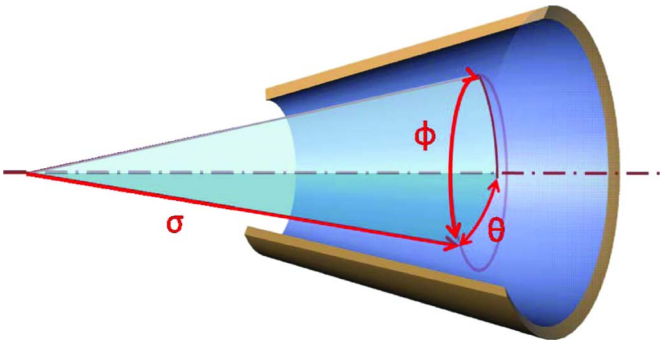

FIG. 2. (Color online) A conic nozzle and the spherical coordinate system used to describe its geometry.

$$\psi(\sigma,0) = \psi_0 \quad \text{and} \quad \psi(\sigma,\theta_w) = \psi_1, \tag{43}$$

where θ_w is the angle between the symmetry axis and the wall. The difference between these two values can be written in terms of the overall "magnetic flow" $\dot{b}$ as

$$\dot{b} \equiv \int_{S_i} \mathbf{B}\cdot d\mathbf{S} = 2\pi\sigma_i^2 \int_0^{\theta_w} B_{\sigma i} \sin(\theta) d\theta = 2\pi(\psi_1 - \psi_0), \tag{44}$$

where S_i is the inlet surface. Since the magnetic flux function is defined modulo an additive constant, we can set the two Dirichlet conditions

$$\psi|_{\theta=0} = 0 \quad \text{and} \quad \psi|_{\theta=\theta_w} = \frac{1}{2\pi}\dot{b}. \tag{45}$$

Together with these conditions, we need to assess the boundary conditions for the open surfaces of the acceleration channel, the inlet, and the outlet surfaces. If we fix a shape of the inlet surface, the boundary condition in the injection region is determined by the way the propellent gas is injected and ionized and, in general, depends on the successive expansion through the nozzle [this is true if the differential operator in the generalized equilibrium equation (18) is locally elliptic]. However, we assume that the plasma attains an extremum of the constrained energy (32) that depends on the injection features only through the shape of the inlet surface. This assumption determines a *natural boundary condition* for the problem. By taking an arbitrary variation $\delta\psi$ at the boundary of the functional (32), we obtain

$$\frac{1}{r^2}(M^2 - 1)\,\nabla\psi\cdot\mathbf{n} = 0, \tag{46}$$

which implies that either the term in the bracket is equal to zero, i.e., the open surface is an Alfvén surface, or that the poloidal magnetic field and mass flow are orthogonal to the open surface. In this way we transfer the indetermination due to the processes that occur before the acceleration channel into the geometry of the domain. A detailed analysis of these processes is outside the scope of the present study; hence, the choice of a suitable inlet surface is in some sense arbitrary and to be based on practical considerations.

The exhaust region presents a similar but more crucial problem since the boundary condition depends on the exter-

nal flow which is unknown. Furthermore, it is clear that the MHD model must cease to be valid at a certain distance in order to permit the detachment of the plasma from the magnetic field that remains linked to the magnetic coils and to the satellite. Again, the natural condition can be used, thus transferring this indetermination into the geometry of the outlet surface. A full analysis of the acceleration channel thus requires a model for the external flow. However, the thrust on the satellite can be exerted only inside the acceleration channel and a reasonable approximation of the natural outlet surface can be sufficient for the purpose of the present analysis. Furthermore, as explained afterward, the normal operation regime implies that $M=1$ in the outlet region close to the wall surface. Consequently, in this region the error due to the surface approximation is small and can be reduced iteratively by correcting the shape of the outlet surface until it coincides with an Alfvén surface.

For the purpose of the present work and numerical investigations, the inlet and outlet surfaces are spherical caps of radius σ_i and σ_o, respectively. The boundary conditions on the two open surfaces result to

$$\left.\frac{\partial \psi}{\partial \sigma}\right|_{\sigma=\sigma_i} = 0 \quad \text{and} \quad (M_o^2 - 1)\left.\frac{\partial \psi}{\partial \sigma}\right|_{\sigma=\sigma_o} = 0. \tag{47}$$

Since Eq. (47) is the natural condition of Eq. (32), in the variational formulation of the problem these equations are implicitly satisfied and do not need to be considered in the numerical implementation of the model.

C. Flux functions

A more delicate analysis is needed in order to choose the functional dependence of the flux functions that, together with the differential equation (18) and the boundary conditions, complete the definition of the problem. A certain degree of freedom is indeed associated with the choice of these functions which characterize different flow regimes. An approximate knowledge of the main fields in the inlet of the acceleration channel is sufficient to obtain a good guess of these dependencies but some constraints follow from physical considerations.

A first simplification consists of the assumption of an isentropic flow, thus $S(\psi)=S_0$. The entropy density depends on the mass injection and plasma generation processes but the isentropic flow represents a reasonable approximation if these occur uniformly before the inlet surface. The overall mass flow rate and poloidal magnetic flux are assigned by the mass supply system and by the external coil circuit. Hence, we can estimate the flux function F as

$$F = \frac{4\pi \dot{m}}{\dot{b}}. \tag{48}$$

A more accurate functional dependence can be determined by approximating the magnetic flux with that produced by the external coil alone

$$\psi_i(\theta) = \frac{\dot{b}}{2\pi}\frac{1-\cos\theta}{1-\cos\theta_w} \tag{49}$$

and by considering the mass flow distribution given by the injection system

$$\dot{m}_i(\theta) = \rho_i v_{\sigma i} A_i, \tag{50}$$

where $A_i = 2\pi\sigma_i^2(1-\cos\theta_w)$ is the area of the inlet surface. Thus, by inverting Eq. (49), we obtain $\theta|_i = \theta(\psi)$ and the expression

$$F(\psi) = \frac{4\pi \dot{m}_i(\psi)}{\dot{b}}. \tag{51}$$

Given an approximation of the azimuthal velocity and magnetic field in the inlet region, the same procedure can be applied to Eqs. (14)–(16) in order to obtain the functional dependencies of G, H, and J on the magnetic flux function. However, we need to solve the differential problem for ψ in order to determine the distribution of the main plasma fields at the inlet surface and verify the consistency of these approximations *a posteriori*.

The electric field can be written as

$$\mathbf{E} = -\frac{1}{c} G \nabla \psi = -\nabla V, \tag{52}$$

where V represents the electric potential. From Eq. (52), we obtain

$$\frac{1}{c}\int_0^{\psi} G(\psi')d\psi' = \Delta V. \tag{53}$$

Since the overall potential difference between the two electrodes ΔV is one of the main parameters of the thruster, it is convenient to introduce the following estimate for G:

$$G = \frac{2\pi c \Delta V}{\dot{b}}, \tag{54}$$

which is exact if the flux function G is a constant.

D. General features of the thruster performance

In order to obtain a thrust, we need to increase the flow velocity through the channel in a divergent nozzle. This implies a sharp decrease of the plasma density and an increase of the Alfvén Mach number ($M^2 = F^2/4\pi\rho$). As described in Ref. 22, the nature of the differential problem changes according to the Alfvén Mach number. In the simple case of a conic magnetic nozzle, the density curve is illustrated in Fig. 2 of Ref. 22. The three transition points correspond to the sound velocity $M=M_a$ and the Alfvén velocity $M=1$, respectively. In the region between these two points, the differential operator in Eq. (18) is elliptic and a solution without a shock discontinuity can be found. In the general case, the region where the generalized equilibrium equation (18) is elliptic is defined by the speeds of the slow and fast magnetosonic waves $M_s \le M \le M_f$. In the inlet region the presence of an azimuthal magnetic field implies that $M_s < M_a$. At the thruster exit, the net current flux is zero and thus the azimuthal magnetic field can be neglected with respect to its

poloidal components. Consequently, the fast magnetosonic speed is equal to the Alfvén velocity and the range $M_a \leq M \leq 1$ can be assumed as the design region for this kind of thruster.

The total current and the voltage difference between the anode and the cathode are the two main design parameters. Given an inlet current distribution $j_{\sigma i}(\theta)$, from Ampére's law we have

$$B_{\phi i} = \frac{4\pi\sigma_i}{c \sin\theta} \int_0^\theta j_{\sigma i} \sin\theta d\theta. \tag{55}$$

At the conductive wall Eq. (55) becomes

$$r_l B_{\phi l} = -2I_{\text{tot}}/c, \tag{56}$$

where the subscript l labels values at the wall leading edge and the total current I_{tot} is considered positive when it flows from the anode to the cathode. We recall the generalized equilibrium equation for the azimuthal magnetic field

$$rB_\phi = \frac{H + r^2 FG}{1 - M^2}. \tag{57}$$

Then we obtain from Eq. (56),

$$I_{\text{tot}} = -\frac{c}{2} \frac{H_w + r_l^2 F_w G_w}{1 - M_l^2}, \tag{58}$$

where M_l^2 is the Alfvén Mach number at the leading edge of the wall and the subscript w indicates that the flux functions, which are constants on the whole anode/wall surface, are evaluated at $\psi = \psi_w$. Since all the current flows from the wall through the inlet surface, the integral of the current density across the outlet surface is zero. Thus, we obtain the condition

$$B_{\phi t} = 0, \tag{59}$$

where the subscript t labels values at the trailing edge of the wall. Using Eq. (57), the above condition on the total current can be rewritten as

$$H_w + r_t^2 F_w G_w = 0, \tag{60}$$

where r_t is the radius of the trailing edge of the wall. In order to avoid the singularity in Eq. (57), the following regularity condition is imposed on Alfvén surfaces

$$H + r^2 FG = 0 \tag{61}$$

and, if $M = 1$ somewhere along the wall, Eq. (60) implies that

$$r|_{M=1} = r_t. \tag{62}$$

The total current that passes through the inlet surface comes from the $M < 1$ part of the anode wall, and thus the Alfvén velocity represents a limit for the plasma velocity in the acceleration channel.

From Eq. (60), it follows that $H_w = -r_t^2 F_w G_w$, and by substituting this expression into Eq. (58), we obtain

$$I_{\text{tot}} = \frac{c}{2} F_w G_w \frac{r_t^2 - r_l^2}{1 - M_l^2}. \tag{63}$$

Introducing a coordinate q at the wall along the axial direction and defining the current $I(q)$ which passes through each section of the channel and the corresponding Mach number M_q, Eq. (63) can be generalized as

$$I(q) = \frac{c}{2} F_w G_w \frac{r_t^2 - r_q^2}{1 - M_q^2}. \tag{64}$$

From Eq. (15), the flux function H evaluated at the leading and trailing edges of the conductive wall is given by

$$H_w = -2I_{\text{tot}}/c - F_w r_l v_{\phi l} = -F_w r_t v_{\phi t}, \tag{65}$$

where we used Eqs. (57) and (59) to eliminate the azimuthal magnetic field. This expression can be rewritten as

$$I_{\text{tot}} = \frac{c}{2} F_w [\![r v_\phi]\!]_w, \tag{66}$$

where $[\![\cdots]\!]_w$ indicates the difference between the values assumed at the trailing and the leading edges of the conductive wall. Moreover, Eq. (14) evaluated at the trailing edge of the wall yields $G_w = v_{\phi t}/r_t$ and, by substituting this expression into Eq. (63), we obtain

$$\frac{v_{\phi t}}{v_{\phi l}} = \frac{r_t}{r_l}(1 - M_l^2)\left(1 - \frac{r_t^2}{r_l^2} M_l^2\right)^{-1}. \tag{67}$$

If we consider the case $G = \text{const}$ and $F = \text{const}$, Eq. (63) becomes

$$I_{\text{tot}} = \frac{4\pi^2 c^2 \dot{m}}{\dot{b}^2} \frac{r_t^2 - r_l^2}{1 - M_l^2} \Delta V, \tag{68}$$

where we have used expressions (48) and (54). As illustrated in Sec. I, the Alfvén Mach number in the inlet region depends on the current I_{tot}. However, we can define a conductance K,

$$K \equiv \frac{4\pi^2 c^2 \dot{m}}{\dot{b}^2} \frac{r_t^2 - r_q^2}{1 - M_q^2}, \tag{69}$$

which characterizes the performances of the thruster. For the divergent nozzle considered in the present analysis, the term $r_t^2 - r_q^2$ is always positive and the Alfvén Mach number in the design range satisfies the condition $M_s^2 \leq M_q^2 < 1$. Therefore, the sign of K is positive and, given a potential $\Delta V > 0$, the energy $I_{\text{tot}} \Delta V$ is transferred to the fluid.

IV. NUMERICAL SOLUTIONS

In order to solve the generalized equilibrium equation, where the two variables v_ϕ and ρ are connected to the magnetic flux function by Eqs. (14) and (16), we exploit the variational formulation (32).

A. Numerical procedure

By reducing the solution space to a subspace with finite dimensions defined by a set of base functions $\mathcal{F}_n$, $\mathcal{G}_m$, and $\mathcal{H}_l$, the three unknown variables are expressed in terms of three truncated series

$$\psi = \sum_{n=0}^{n_T} \psi_n \mathcal{F}_n, \quad \rho = \sum_{m=0}^{m_T} \rho_m \mathcal{G}_m, \quad v_\phi = \sum_{l=0}^{l_T} v_{\phi l} \mathcal{H}_l. \tag{70}$$

Then, the functional (32) reduces to a function of the three sets of coefficients $\mathbf{x}=[\psi_n, \rho_m, v_{\phi l}]$. An extremum belonging to the solution space can be found by setting the derivatives of $\mathcal{L}$ with respect to the coefficients of these series equal to zero. The solution of the system of nonlinear equations

$$\mathbf{f}(\mathbf{x}) = 0, \quad \text{where } f_i = \frac{\partial \mathcal{L}}{\partial x_i}, \tag{71}$$

is then found using the Newton–Raphson method[33] or one of its variants so that the continuity of the functional and of its derivatives is exploited. The iterative solution

$$\mathbf{x}^{i+1} = \mathbf{x}^i - \mathbf{J}^{-1}(\mathbf{x}^i)\mathbf{f}(\mathbf{x}^i) \tag{72}$$

is written in terms of the Jacobian

$$J_{ij} = \frac{\partial f_i}{\partial x_j} = \int_V \frac{\partial}{\partial x_j}\left(\frac{\partial L}{\partial x_i}\right) d^3 r = J_{ji}, \tag{73}$$

where the function $L(\mathbf{x})$ follows from Eq. (32). For $M_s^2 \le M^2 \le 1$, the elliptic nature of the equation guarantees the well posedness of the problem. Moreover, natural boundary condition is automatically satisfied by the extremization process.

The set of base functions can be defined on the whole integration region or on the elements of a domain triangulation [finite elements, finite elements method (FEM)]. The solutions presented in Sec. IV B are obtained by using the FEM approach, which permits more flexibility on the domain definition and better accuracy for nonsmooth solutions. Moreover, this approach can be implemented by using dedicated programming languages that guarantee an optimization of the numerical routines and good time performance. In the present case the numerical code was implemented by using the FreeFem++ software. The numerical algorithm can be easily adapted to parallel computing.

B. Results

The numerical investigations of the plasma flow in the applied-field MPD thruster are performed for the simple conic nozzle configuration introduced in Sec. II. The characteristic dimensions of the configuration and the typical values of the mass flow rate and poloidal magnetic flux are deduced from Refs. 28 and 29 and represent the assigned parameters of the problem. Then, the functional dependencies of the flux functions F, G, H, and J need to be defined. As discussed in Sec. III, these dependencies can be assigned on the basis of an estimate of the main plasma quantities in the inlet region. However the correctness of this estimate needs to be justified *a posteriori* as shown in the numerical simulations presented hereafter.

We start by taking the poloidal magnetic field at the inlet surface to be the "vacuum field." Then the magnetic flux function is given by Eq. (49), which can be rewritten as

$$\psi_i = \psi^*(1 - \cos\theta), \tag{74}$$

where $\psi^* = \dot{b}/[2\pi(1-\cos\theta_w)]$. Next, we consider uniform inlet conditions for the plasma density and velocity. Hence, the flux function F is a constant and, as obtained in Eq. (48), it is equal to $F = 4\pi\dot{m}/\dot{b}$. Then we consider the following inlet conditions for the azimuthal velocity and magnetic field:

$$v_{\phi i} = \alpha r, \quad B_{\phi i} = \beta r, \tag{75}$$

where the parameter α represents the inlet angular velocity that is assumed to be uniform, while the parameter β can be expressed in terms of the total current as $\beta = -2I_{\text{tot}}/cr_l^2$. These conditions correspond to a constant flux function G, which from Eq. (54) takes the form

$$G = \alpha - \beta M_i^2/F = \frac{2\pi c}{\dot{b}}\Delta V. \tag{76}$$

Similarly, the flux function H defined by Eq. (15) can be rewritten in the form

$$H = r^2(\beta - \alpha F) = \sigma_i^2(\beta - \alpha F)\frac{\psi}{\psi^*}\left(2 - \frac{\psi}{\psi^*}\right), \tag{77}$$

where the relationship $r|_i = \sigma_i \sin\theta$ and Eq. (74) have been used. Moreover, from the current condition given by Eq. (59), we obtain the constraint

$$\beta - \alpha F = -\frac{2\pi c}{\dot{b}}\frac{r_t^2}{r_l^2}F\Delta V, \tag{78}$$

which is equal to Eq. (68) and, substituted into Eq. (77), yields

$$H = -\sigma_o^2\frac{2\pi c}{\dot{b}}F\Delta V\frac{\psi}{\psi^*}\left(2 - \frac{\psi}{\psi^*}\right). \tag{79}$$

The generalized Bernoulli function J given by Eq. (16) becomes

$$J = \frac{1}{2}\left(\frac{\psi^* M_i}{\sigma_i^2 F}\right)^2\left(M_i^2 + \frac{2}{\gamma - 1}M_{si}^2\right) + \sigma_i^2(2\alpha\beta M_i^2/F - \alpha^2)\frac{\psi}{\psi^*}\left(2 - \frac{\psi}{\psi^*}\right), \tag{80}$$

where $M_{si} = \sqrt{4\pi\gamma p_i \sigma_i^4/\psi^*}$ is the ratio between the inlet sound velocity $v_{si} = \sqrt{\gamma p_i/\rho_i}$ and the Alfvén velocity $v_{ai} = \psi^* M_i/(\sigma_i^2 F)$. The isentropic relationship between the pressure and the plasma density $p = p(\rho)$ can be deduced from the injection and ionization conditions, and thus M_s turns out to be a function of the plasma density or, since $\rho_i = F^2/4\pi M_i^2$, of the inlet Alfvén Mach number.

The obtained description depends on the potential difference ΔV and the inlet Alfvén Mach number M_i. However, for the simple model described in Sec. IV, these two parameters are dependent and thus we may expect that a similar dependence exists in the case considered here. This implies that, given both the potential difference ΔV and the inlet Alfvén

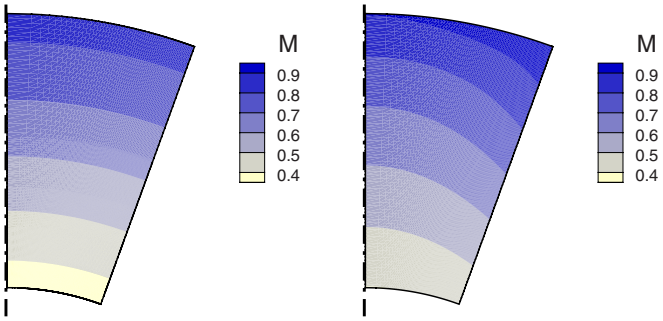

FIG. 3. (Color online) Left frame: Alfvén Mach number of the plasma flow in a conic magnetic nozzle with potential difference $\Delta V=0$ and inlet flow velocity equal to the sound speed. Right frame: Alfvén Mach number for the optimal condition (i.e., when the plasma velocity at the trailing edge of the anode wall is equal to the Alfvén velocity). The dimensionless value of the potential difference is $\Delta V=0.37$.

Mach number M_i, the problem is overconstrained and, in general, the estimates made in order to define the functional dependencies of the flux functions are not in full agreement with the obtained solution. A way to partially overcome this problem is to adapt the value of M_i in the expression (80) through an iterative procedure. We start with an initial guess of the value of M_i and find a solution of the nonlinear problem (71), then the value and the behavior of the inlet Alfvén Mach number obtained from this solution is compared with the initial guess. A new value for the inlet Alfvén Mach number is deduced from this comparison and the nonlinear system of Eq. (71) is solved until the difference between two successive solutions is small enough.

In the case of $\Delta V=0$, an analytic solution of the generalized equilibria equations exists and is presented in Ref. 22. This peculiar case, which corresponds to a purely hydrodynamic expansion of the plasma in a magnetic nozzle, can be used as an initial approximation of the solution in the numerical investigation of the complex electromagnetic configurations that characterize the thruster. In particular, if the applied potential difference is zero, the magnetic flux function is that of the vacuum field [Eq. (49), the plasma density is a function of σ, and the thrust is only due to the thermodynamic effect of the nozzle expansion. In Fig. 3, left frame, the Alfvén Mach number in the channel, which in this case depends on the spherical radius σ only, is shown. We notice that in this case the outgoing kinetic power P_{k0} can be approximated as

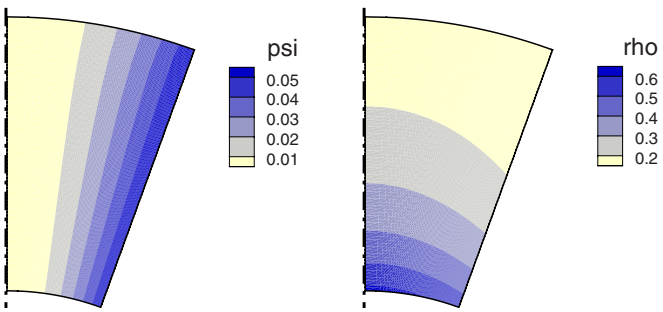

FIG. 4. (Color online) Magnetic flux function ψ and plasma density ρ in dimensionless units for the optimal conditions.

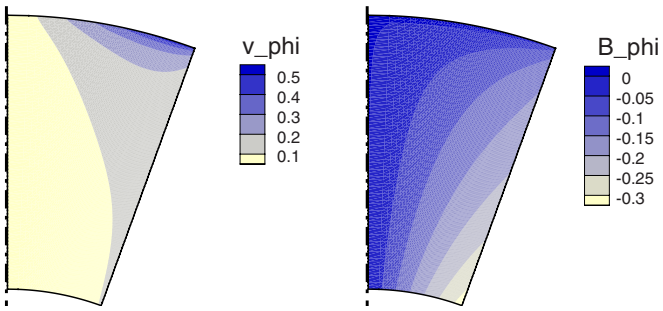

FIG. 5. (Color online) Azimuthal plasma velocity v_ϕ and magnetic field B_ϕ in dimensionless units for the optimal conditions.

$$P_{k0} \approx \frac{\dot{b}^2}{A_o^2}\frac{\dot{m}}{2F^2}M_{t0}^4, \tag{81}$$

where $M_{t0}\approx 0.85$ is the value of the Alfvén Mach number at the outlet surface and $A_o=2\pi\sigma_o^2(1-\cos\theta_w)$ is the area of the outlet surface. Then, we consider a small increment of the potential difference and we solve the problem with the initial guess value of M_i given by the case $\Delta V=0$. By increasing the potential difference, the electromagnetic power contribution to the plasma acceleration is of order

$$I_{\text{tot}}\Delta V = \frac{4\pi^2 c^2 \dot{m}}{\dot{b}^2}\frac{r_t^2 - r_l^2}{1-M_i^2}\Delta V^2. \tag{82}$$

Since the optimal condition is reached for $M_t=1$, the increase of the outgoing kinetic power $\Delta P_k \equiv P_{k,\text{opt}} - P_{k0}$ can be written as

$$\Delta P_k \approx \frac{\dot{b}^2}{A_o^2}\frac{\dot{m}}{2F^2}(1-M_{t0}^4). \tag{83}$$

Equating $I_{\text{tot}}\Delta V$ in Eq. (82) and ΔP_k in Eq. (83) and using the relationships $r_{t,l}=\sigma_{o,i}\sin\theta_w$, we obtain

$$\frac{\Delta V}{\widetilde{\Delta V}} \approx \left[\frac{(1-M_i^2)}{(\sigma_o/\sigma_i)^2-1}\frac{(1-M_{t0}^4)}{\sin^2\theta_w}\left(\frac{\sigma_i}{\sigma_o}\right)^4\right]^{1/2}, \tag{84}$$

where the parameter

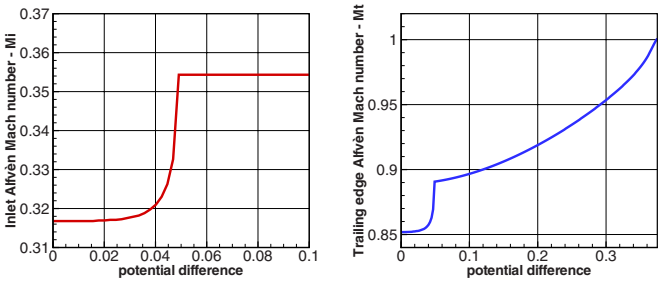

FIG. 6. (Color online) Left frame: inlet Alfvén Mach number M_i as a function of ΔV near the threshold value $\Delta V^*\approx 0.05$. Right frame: Alfvén Mach number M_t at the trailing edge of the anode wall as a function of ΔV.

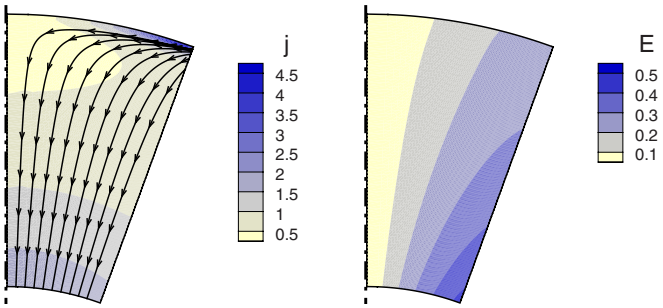

FIG. 7. (Color online) Left frame: the dimensionless poloidal current density $|\mathbf{j}_p|$ together with the current streamlines. Right frame: the electric field in dimensionless units for the optimal condition.

$$\widetilde{\Delta V} = \frac{\dot{b}^3}{8\pi^2 \dot{m}} \frac{1}{\sqrt{2} c \sigma_i A_i}$$

is adopted as a natural scale of the potential difference. Taking $M_i \approx M_s$, the estimate of the dimensionless potential difference for the optimal condition gives $\Delta V/\widetilde{\Delta V} \approx 0.3$.

As illustrated in Figs. 3–5, the flow depends on the two poloidal coordinates and a clear effect of the electromagnetic plasma acceleration is the decrease of the density at the anode surface. By increasing the applied potential difference, the Alfvén Mach number at the inlet M_i must be increased (see Fig. 6) in order to guarantee the agreement with the described estimate. However, as a consequence of the density decrease near the wall, above the threshold value $\Delta V^* \approx 0.05$ the density in the inlet region is not uniform and the previous estimate cannot be improved by adjusting the single parameter M_i. Nonetheless, the solution for the assigned flux functions can be found until the optimal thruster operation is reached (the optimal condition corresponds to the simulation results reproduced in Figs. 3–5). In Fig. 6 the Alfvén Mach number at the trailing edge of the wall is presented for different values of the potential difference. For $\Delta V \leq \Delta V^*$, the inlet Alfvén Mach number is adapted to the initial estimate. For larger values of the potential difference, M_i is taken constant. The current density is presented in Fig. 7 together with the current streamlines. It is clear from this picture that the current density concentrates in the region of the anode wall near the exit of the acceleration channel. We recall that the electric potential is constant on the flux surfaces, which are shown in Fig. 4 and, consequently, the electric field (see Fig. 7) is almost along the θ direction.

As can be expected from the analysis of the problem and, in particular, from Eq. (62), if the plasma velocity at the wall become greater than the Alfvén speed, $M > 1$, the numerical algorithm diverges and no solution can be found. This condition represents a new limit to the ideal thruster operation.

V. CONCLUSIONS

The ideal MHD description of the plasma flow represents a valuable framework in order to understand the main acceleration processes in an applied-field MPD thruster. Moreover, the MHD model allows us to define the limits of ideal, axial symmetric, and steady state operations of the thruster, which marks the onset of a different flow regime. A first "onset" condition is deduced as a limit on the inlet velocity, which is bounded by the ionization process of the propellant gas. Then, the requirement that the net current flow at the outlet surface is zero yields a current-tension relationship and the definition of an optimal condition for the ideal thruster operations, which thus provide useful design strategies.

The variational formulation of the problem has been implemented numerically using a finite element approach that proved to be efficient and in perfect agreement with previously reported results. The numerical simulations offer good examples of the flow behavior and, in particular, show the relationships with the input electromagnetic power that characterize the onset of critical regimes and also the mass starvation problems at the anode.

As mentioned before, the approach used in the present paper can be extended to different plasma configurations with flows provided one can assume that the configuration is stationary and axisymmetric. In particular, the numerical approach described in Sec. IV that is based on the variational principle can be easily extended to the study of astrophysical jets and of fusion plasma equilibria with flows. Similarly, the relationships between the applied potential and the plasma current derived in Sec. III can be suitably generalized.

Finally, the Hamiltonian formulation on which the variational principle is based provides a general tool for addressing stability issues, which also represent a critical feature of the MPD thrusters (see Refs. 34 and 35 and references therein) and that will be the object of future investigations.

[1] R. G. Jahn, *Physics of Electric Propulsion* (McGraw-Hill, New York, 1968).
[2] H. Grad and H. Rubin, *Proceedings of Second United Nations International Conference on the Peaceful Uses of Atomic Energy* (United Nations, Geneva, 1958), Vol. 31, pp. 190–197.
[3] V. D. Shafranov, in *Reviews of Plasma Physics*, edited by M. A. Leontovich (Consultants Bureau, New York, 1966), Vol. 2, pp. 103–151.
[4] R. Lüst and A. Schlüter, Z. Astrophys. **34**, 263 (1954).
[5] S. L. Bragg and W. R. Hawthorne, J. Aero. Sci. **17**, 243 (1950).
[6] R. R. Long, J. Meteorol. **10**, 197 (1953).
[7] H. B. Squire, in *Surveys in Mechanics*, edited by G. K. Batchelor and R. M. Davies (Cambridge University Press, Cambridge, 1956), pp. 139–161.
[8] A. R. Elcrat and K. G. Miller, Diff. Integral Eq. **16**, 949 (2003).
[9] H. A. Scott and R. V. E. Lovelace, Astrophys. J. **252**, 765 (1982).
[10] R. V. E. Lovelace, C. Mehanian, C. M. Mobarry, and M. E. Sulkanen, Astrophys. J., Suppl. Ser. **62**, 1 (1986).
[11] J. P. Goedbloed, Phys. Plasmas **11**, L81 (2004).
[12] J. P. Goedbloed, Phys. Plasmas **15**, 062101 (2008).
[13] P. J. Morrison and J. M. Greene, Phys. Rev. Lett. **45**, 790 (1980); **48**, 569 (1982).
[14] P. J. Morrison, AIP Conf. Proc. **88**, 13 (1982).
[15] R. Salmon, Annu. Rev. Fluid Mech. **20**, 225 (1988).
[16] P. J. Morrison, Rev. Mod. Phys. **70**, 467 (1998).
[17] P. J. Morrison, Phys. Plasmas **12**, 058102 (2005).
[18] M. Heinemann and S. Olbert, J. Geophys. Res. **83**, 2457, doi:10.1029/JA083iA06p02457 (1978).
[19] E. Hameiri, Phys. Plasmas **5**, 3270 (1998).
[20] E. Hameiri, Phys. Plasmas **11**, 3423 (2004).
[21] T. Andreussi, P. J. Morrison, and F. Pegoraro, Plasma Phys. Controlled Fusion **52**, 055001 (2010).
[22] T. Andreussi and F. Pegoraro, Phys. Plasmas **15**, 092108 (2008).
[23] R. D. Blandford and D. G. Payne, Mon. Not. R. Astron. Soc. **199**, 883 (1982).

[24]J. Contopoulos, Astrophys. J. **450**, 616 (1995).
[25]J. Contopoulos, Astrophys. J. **460**, 185 (1996).
[26]P. M. Bellan, S. You, and S. C. Hsu, Astrophys. Space Sci. **298**, 203 (2005).
[27]L. Guazzotto and R. Betti, Phys. Plasmas **12**, 056107 (2005).
[28]F. Paganucci, P. Rossetti, M. Andrenucci, V. B. Tikhonov, and V. A. Obukhov, *Proceedings of the 27th International Electric Propulsion Conference*, Pasadena, CA, 2001 (Electric Rocket Propulsion Society, Fairview Park, 2001).
[29]M. Zuin, R. Cavazzana, E. Martines, G. Serianni, V. Antoni, M. Bagatin, M. Andrenucci, F. Paganucci, and P. Rossetti, Phys. Rev. Lett. **92**, 225003 (2004).
[30]J. P. Goedbloed and S. Poedts, *Principles of Magnetohydrodynamics* (Cambridge University Press, Cambridge, 2004), pp. 208–211.
[31]H. Maecker, Z. Phys. **141**, 198 (1955).
[32]E. Choueiri, J. Propul. Power **14**, 744 (1998).
[33]P. Deuflhard, *Newton Methods for Nonlinear Problems* (Springer-Verlag, Berlin, 2004).
[34]M. Zuin, R. Cavazzana, E. Martines, G. Serianni, V. Antoni, M. Bagatin, M. Andrenucci, F. Paganucci, and P. Rossetti, Phys. Plasmas **11**, 4761 (2004).
[35]F. Paganucci, M. Zuin, M. Agostini, M. Andrenucci, V. Antoni, M. Bagatin, F. Bonomo, R. Cavazzana, P. Franz, L. Marrelli, P. Martin, E. Martines, P. Rossetti, G. Serianni, P. Scarin, M. Signori, and G. Spizzo, Plasma Phys. Controlled Fusion **50**, 124010 (2008).